SSC-SDE-22

SSC-SDE
SOLENOIDAL DETECTOR NOTES

POSITIVE ION DISTORTIONS IN WARM LIQUID CALORIMETERS
1 November 1989

R. W. Kadel

POSITIVE ION DISTORTIONS IN WARM LIQUID CALORIMETERS

R.W. Kadel
Lawrence Berkeley Laboratory
November 1, 1989

Abstract

We have calculated the distortions due to positive ions for an organic liquid calorimeter and found the effects less than 0.1% at luminosities of 10^{33} in TMS, in contrast to published data which implies effects of order 1% near the beam line.

Introduction

The charge deposited in an organic liquid calorimeter depends on the static value of the electric field and to first order is described by the Onsager relation:

$$\frac{dQ}{dz} = k_1 + k_2 E \tag{1}$$

Anderson[1], et al., have shown that, to the accuracy of the Onsager relation, the total charge *deposited* in an organic liquid depends on the applied voltage and the width of the gap, but is independent of the rate of incoming ionization. The charge *integrated* by an amplifier, however is sensitive to the spatial distribution of the deposited charge, and to the extent that positive ions distort the static electric field, the charge seen by an amplifier will have a rate dependence. At the high rate environment of the SSC it is possible that the ionization near shower maximum in an organic liquid ionization electromagnetic calorimeter is so intense as to the change the static electric field and thereby modify the charge seen at the output. For a useful electromagnetic calorimeter this change in the output should be much less than 1%. Anderson, et al., have published data indicating that at luminosities of 10^{33} cm^{-2} sec^{-1} the response of an organic liquid calorimeter could change by as much as a few percent at pseudo-rapidities of 2.5 or greater. Figures 1 and 2 are reproduced from their paper. As can be seen, at fluxes corresponding to 10^7 particles per cm^2, there should be changes in the response of order a few percent.

Background

We first sought to verify the rates calculated in the paper. Let F be the flux of particles, A the area of the detector, I the current and L the length of the gap. Then we invoke charge

conservation:

$$\text{Charge out} = \text{Charge in}$$

$$I = AFL(k_1 + k_2 E), \tag{2}$$

or

$$F = \frac{I}{AL(k_1 + k_2 E)} \text{ tracks per unit area,} \tag{3}$$

where k_1 and k_2 are the Onsager constants for TMS and E is the electric field in the gap. Using Figure 1 from the Anderson paper we estimate that a target current of 6.5×10^{-7} amp equals a cell current of 4.5×10^{-8} amp, from which we can calculate an equivalent flux of

$$F = \frac{45 \times 10^{-9} \text{ Amp}}{1.77 \times 10^{-4} m^2 \times 1.0 \times 10^{-3} m \times (1.6 \times 10^{-13} C/m + .96 \times 10^{-19} C/V \times 1 \times 10^{6} \text{ V/m})} \tag{4}$$

$$= 10^{8} \text{ tracks/cm}^2 \text{ at shower maximum} \tag{5}$$

This is a factor of 10 greater than the value listed in the upper scale of Figure 2 for this target current. If we use the model for the number of tracks at shower maximum as a function of rapidity given in Reference 1, we conclude that this rate corresponds to a Luminosity of 10^{34} $\text{cm}^2\text{sec}^{-1}$ at pseudo-rapiditys of $\eta = 3.0$ for a shower counter 2 meters downstream of the interaction point. The response calculated in by Anderson is therefore appropriate for the SSC at a luminosity of *at least* 10^{34}.

Since the resolution of the electromagnetic calorimeter should be 1% or better, and it is hard to measure small systematic effects in a test beam setup, we undertook to see if we could calculate the variation of the response of such a calorimeter as a function of the electric field, the detector gap width, the detector geometry and the luminosity in order to predict the behavior at high rates.

Theory

As mentioned above, the ionization deposited in an organic liquid depends on the applied electric field and can be approximated by the Onsager relation

$$\frac{dJ}{dz} = F(k_1 + k_2 E) \tag{6}$$

where J is the (linear) current density and E is the applied electric field. In the case of TMS we can substitute the measured values of k_1 and k_2 to discover $\frac{dJ}{dz} = F(1.0 \times 10^6 + 0.6E)$ ions/meter, where E is measured in Volts per meter. The charge density (ρ) is related to the current density by

$$J = \rho V \tag{7}$$

where V is the ion drift velocity. The drift velocity of the ions is very slow, about 5 cm/sec at 10 KV/cm electric fields. From Maxwell's equations we also have the relation between E and ρ:

$$\frac{dE}{dz} = \frac{\rho}{\epsilon} \tag{8}$$

where ϵ is the permitivity of the medium and z is the spatial coordinate. Combining these last three equations and recalling that the ion drift velocity is proportional to the electric field (i.e., $V = \mu E$) we find:

$$\frac{\epsilon\mu}{2}\frac{d^2(E^2)}{dz^2} = F(k_1 + k_2 E), \tag{9}$$

a non-linear equation we do not know how to solve.

In order to proceed further, we rewrite equation (6) for the linear current density as:

$$\frac{dJ}{dz} = F\alpha, \tag{10}$$

were α is a constant equal to the ionization/meter given by the Onsager relation for the nominal value of the electric field. We then obtain the following first order equation for E:

$$EdE = \frac{F\alpha z dz}{\mu\epsilon} \tag{11}$$

from which we find

$$E = \beta\sqrt{(z^2 + \gamma^2)} \tag{12}$$

where $\beta^2 = F\frac{\alpha}{(\mu\epsilon)}$ and γ is a constant to be determined from the boundary conditions. Integrating to find the potential $\Phi(z)$ we have:

$$\Phi(z) = -\beta\left\{\frac{z}{2}\sqrt{z^2+\gamma^2} + \frac{\gamma^2}{2}\log(z + \sqrt{z^2+\gamma^2}\right\} + \text{const} \tag{13}$$

The value of the integration constant and γ are determined from the boundary conditions:

$$\begin{array}{lll} \Phi(z) = \Phi_0 & \text{at} & z = 0 \\ \Phi(z) = 0 & \text{at} & z = L \end{array} \tag{14}$$

From which we obtain the following equation for γ:

$$\Phi_0 = \frac{\beta\gamma^2}{2}\log\left(\frac{\gamma}{L + \sqrt{L^2+\gamma^2}}\right) - \frac{\beta L}{2}\sqrt{L^2+\gamma^2} \tag{15}$$

This transcendental equation can be solved numerically.

In a parallel plate ionization calorimeter, the image charge (dQ) collected by an amplifier from a charge (dQ') deposited at distance z in the gap is given by:

$$dQ = \frac{z}{L} dQ'. \tag{16}$$

We can use this relation to calculate the total charge seen by the amplifier by recalling that $dQ' = F\alpha dz$, where α is a function of the modified electric field:

$$Q = \int_0^L \frac{z}{L} F\alpha dz \tag{17}$$

$$= \int_0^L \frac{z}{L} F(k_1 + k_2 E) dz \tag{18}$$

Once we have numerically calculated the constant γ in the formula (10) for the electric field we can calculate the total charge seen by an amplifier:

$$Q = \int_0^L \frac{z}{L} F(k_1 + k_2 \beta \sqrt{z^2 + \gamma^2}) dz \tag{19}$$

$$= F\left(\frac{k_1 L}{2} + \frac{k_2 \beta}{3L}\left(\sqrt{L^2 + \gamma^2}^3 - \gamma^3\right)\right). \tag{20}$$

This should be compared to the expected result

$$Q_0 = F\left(\frac{k_1 L}{2} + \frac{k_2 E_0 L}{2}\right), \quad \text{where} \quad E_0 \equiv \frac{\Phi_0}{L}. \tag{21}$$

If we label the non-linear response ($Q - Q'$) as ΔQ, then

$$\frac{\Delta Q}{Q_0} = \frac{\left[\frac{L k_2 E_0}{2} - \frac{k_2 \beta}{3L}\left(\sqrt{l^2 + \gamma^2}^3 - \gamma^3\right)\right]}{\left(\frac{k_1 L}{2} + \frac{k_2 E_0 L}{2}\right)}. \tag{22}$$

Low Rate Behavior

It is also interesting to look at equation (12) for the electric field in the limit of low ionization densities. In the limit of low rates (i.e. $\beta \to 0$), one can show that $\gamma \to \frac{\Phi_0}{(\beta L)}$ or $E \to \frac{\Phi_0}{L}$ as expected. Near this limit the electric field is given by:

$$E = E_0 - \frac{(\beta L)^2}{6E_0} + \frac{(\beta z)^2}{2E_0} \tag{23}$$

the charge density ρ, given by $\epsilon(dE/dz)$ is then

$$\rho = \frac{\epsilon \beta z}{E_0}, \tag{24}$$

and is seen to vary linearly across the gap.

The total charge collected by an amplifier is calculated by the formalism described above and is given by:

$$Q = \int_0^L \frac{z}{L} F \left\{ k_1 + k_2 \left[E_0 - \frac{(\beta L)^2}{6E_0} + \frac{(\beta z)^2}{2E_0} \right] \right\} dz \tag{25}$$

Integrating over the gap, we find

$$Q = F \left\{ \frac{k_1}{2} + \frac{k_2 E_0}{2} + \frac{k_2 L^3 \beta^2}{24 E_0} \right\}. \tag{26}$$

The first two terms inside the curly brackets represents the charge we would normally expect to get (Q_0), while the last term is the non-linearity to positive ion distortion. Again, calling this term ΔQ, we can calculate the ratio of the non-linear part to the linear part recalling that $\beta^2 = \frac{F\alpha}{\mu\epsilon} = \frac{F(k_1 + k_2 E)}{\mu\epsilon}$.

$$\frac{\Delta Q}{Q_0} = \frac{k_2 F L^2}{(12 \mu\epsilon E_0)}. \tag{27}$$

This shows that the non-linearity grows as the square of the gap, and is inversely proportional to the electric field (or the positive ion drift velocity if we combine μE_0 to form V, the ion drift velocity). In the Anderson setup, the non-linearity is seen to grow as the electric field grows, a discrepancy we are unable to resolve.

Numerical Results

We have written a short computer program which numerically calculates the value of γ, given the luminosity, gap width, nominal electric field and detector η. For an incident flux on the test cell of $10^7/\text{cm}^2$ at an electric field of 20KV/cm and found that the change in collected charges (ΔQ)is of order 10^{-4} of the naive prediction (Q_0). Table I and Figure 4 give the results as a function of η for the SSC detector shown in Figure 3. In Table 2 and Figure 5 we calculate the result as a function of the rate of tracks, independent of any particular detector design. As can be seen, even at the highest rates conceivable at the SSC (i.e., 10 times design luminosity) we do not expect to see large departures from linearity.

Discussion and Conclusions

We have tried to present a model for the rate dependence of an organic liquid calorimeter and found that at typical SSC rates near the beam line the nonlinear response of TMS to be a negligible effect. We note that even at higher rates, we have been unable to reproduce the size of

the nonlinear response as measured by Anderson, et al. Referring to Table 5, we observe that at the highest currents measured by Anderson, et al., we would only see a change in the electric field of at most 4%, assuming a uniform flux of min-ionizing tracks that completely penetrated the gap. It is difficult to to see how such a small change in the electric field could lead to 15% nonlinear terms, given the assumptions made here.

The source of the radiation in the Anderson setup were photons produced by a 1.6 MeV electron beam impinging on a tungsten target. Figure 6 shows the absorption cross section for low energy photons. We note the the energy range of 2 KeV, the absorption length is 4×10^{-3} cm. This would imply that the photons are almost completely absorbed at the 'upstream' end of the gap nearest the photon source. If the electric field points in the beam direction, it is possible to get more charge. However, if the electric field points opposite to the beam direction, less charge will be collected. It is also true that a pulsed source was used to make the measurement, with a frequency of 197 hz, and that changes in the flux were induced by changing the intensity rather than the rate of the source. Under these conditions and at the highest electric fields, all of the ions from previous pulses would have been cleared in the time between pulses and we would be looking at the distortions produced by one pulse on the charge collected during that pulse ('self distortions'). Hence, the charge density has not only a spatial dependence but also an unknown time dependent term, and a steady state situation is never achieved on the microscopic level. This might make the results impossible to translate to the environment seen by a SSC detector.

Acknowledgments

I would like to thank M. Binkley, D. Anderson, R. Ely and W. Wenzel for useful discussions.

Reference

1) D.F. Anderson and R.A. Holroyd, NIM, A 260 (1987) 343.

APPENDIX

High Rate Behavior

We note that at high ion densities our approximation to the exact nonlinear response is no longer valid. However, some interesting observations can be made. Considering equation (12) for the electric field vs. z, we notice that when γ vanishes, the electric field vanishes near $z = 0$ and electrons no longer reach the anode. At this point one has the unusual situation where the ionization density is high enough to have canceled the electric field and the electrons at the anode are stagnated and begin to recombine with local ions. The current density in the gap at this point can be calculated by solving equation (15) for β and letting γ approach zero. We find the value of β at which this occurs is:

$$\beta_m = \frac{2\Phi_0}{L^2} = \sqrt{(J_m/\mu\epsilon L)} \tag{28}$$

or

$$J_m = \frac{4\Phi_0^2\mu\epsilon}{L^3} \tag{29}$$

For the Anderson setup, this current is:

$$I_m = J_m A = 2000 \text{ nAmp} \tag{30}$$

and when we compare this value to Figures 1 and 2 we estimate that the incident flux at the highest rates was about 5% I_m calculated in equation (30).

If we use the result for the electric field when the gap shut off (i.e. $E = \beta_m z$) we then find that the non-linearity in this case is given by

$$\frac{\Delta Q}{Q_0} = \frac{1}{3}\frac{k_2 E_0}{(k_1 + k_2 E_0)}, \tag{31}$$

or approximately 20% for electric fields of 20 KV/cm.

TABLE I: Calculated change in collected charge for the SSC (Luminosity = 10^{33}/sec/cm^2) detector of Figure 3. The radius of the barrel em shower counter is assumed to be 2 meters and the face of the endplug electromagnetic calorimeter 4 meters from the interaction point. A voltage of 2 KV has been applied across a gap of 1 mm.

η	radius (m)	F (MIPS/m^2)	β (V/m^2)	γ (m)	$E(z=L)-E_0$ (V/m)	$\frac{\Delta Q}{Q_0}$	Q (electrons)
0.00	2.00	8.85E+07	6.239D+06	3.206D-01	6.531D+00	4.540D-07	1.100D+03
0.20	2.04	1.08E+08	6.885D+06	2.905D-01	7.926D+00	5.458D-07	1.100D+03
0.40	2.16	1.30E+08	7.575D+06	2.640D-01	9.583D+00	6.574D-07	1.100D+03
0.60	2.37	1.57E+08	8.313D+06	2.406D-01	1.154D+01	7.900D-07	1.100D+03
0.80	2.67	1.88E+08	9.107D+06	2.196D-01	1.385D+01	9.512D-07	1.100D+03
1.00	3.09	2.26E+08	9.964D+06	2.007D-01	1.655D+01	1.130D-06	1.100D+03
1.20	3.62	2.70E+08	1.089D+07	1.836D-01	1.984D+01	1.364D-06	1.100D+03
1.40	4.30	3.22E+08	1.191D+07	1.680D-01	2.363D+01	1.612D-06	1.100D+03
1.60	4.34	5.43E+08	1.546D+07	1.294D-01	3.986D+01	2.727D-06	1.100D+03
1.80	4.22	9.95E+08	2.092D+07	9.559D-02	7.297D+01	4.979D-06	1.100D+03
2.00	4.15	1.81E+09	2.820D+07	7.093D-02	1.325D+02	9.035D-06	1.100D+03
2.20	4.10	3.26E+09	3.789D+07	5.277D-02	2.393D+02	1.632D-05	1.100D+03
2.40	4.07	5.87E+09	5.084D+07	3.933D-02	4.308D+02	2.939D-05	1.100D+03
2.60	4.04	1.06E+10	6.814D+07	2.935D-02	7.738D+02	5.276D-05	1.100D+03
2.80	4.03	1.89E+10	9.128D+07	2.190D-02	1.388D+03	9.467D-05	1.100D+03
3.00	4.02	3.40E+10	1.222D+08	1.635D-02	2.489D+03	1.698D-04	1.100D+03

TABLE II: Calculated change in charge collected as a function of the rate of minimum ionizing particles per sec per cm^2. A potential of 2 KV has been applied across a gap of 1 mm.

F (mips/m^2)	β (V/m^2)	γ (m)	$E(z=L)-E_0$ (V/m)	$\frac{\Delta Q}{Q_0}$	Q (electrons)
1.00E+10	6.634D+07	3.014D-02	7.333D+02	-4.528D-06	1.100D+03
2.00E+10	9.382D+07	2.131D-02	1.466D+03	4.548D-05	1.100D+03
4.00E+10	1.327D+08	1.506D-02	2.932D+03	1.455D-04	1.100D+03
8.00E+10	1.876D+08	1.064D-02	5.861D+03	3.454D-04	1.100D+03
1.60E+11	2.653D+08	7.515D-03	1.171D+04	7.450D-04	1.101D+03
3.20E+11	3.753D+08	5.298D-03	2.336D+04	1.544D-03	1.102D+03
6.40E+11	5.307D+08	3.724D-03	4.651D+04	3.138D-03	1.103D+03
1.28E+12	7.505D+08	2.602D-03	9.219D+04	6.317D-03	1.107D+03
2.56E+12	1.061D+09	1.795D-03	1.813D+05	1.264D-02	1.114D+03
5.12E+12	1.501D+09	1.206D-03	3.514D+05	2.514D-02	1.128D+03
1.02E+13	2.123D+09	7.599D-04	6.662D+05	4.980D-02	1.155D+03
2.05E+13	3.002D+09	3.938D-04	1.226D+06	9.874D-02	1.209D+03

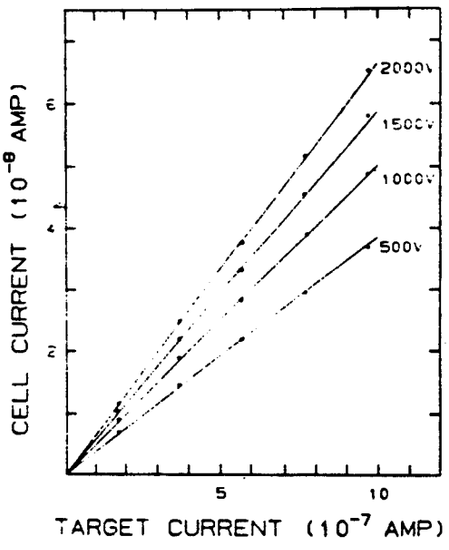

Fig. 1. Cell current as a function of target current for four collection voltages. (Ref 1)

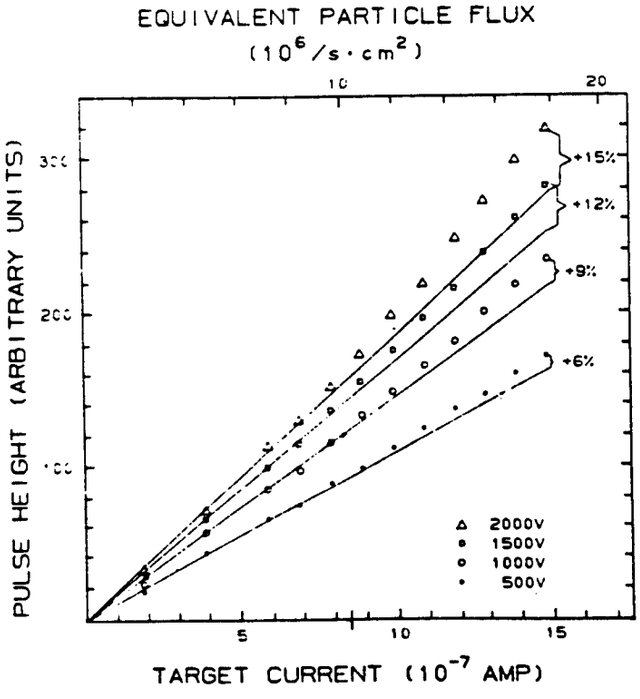

Fig. 2. Pulse height as a function of target current and as a function of equivalent particle (electron–positron) flux for four collection voltages. (Ref 1)

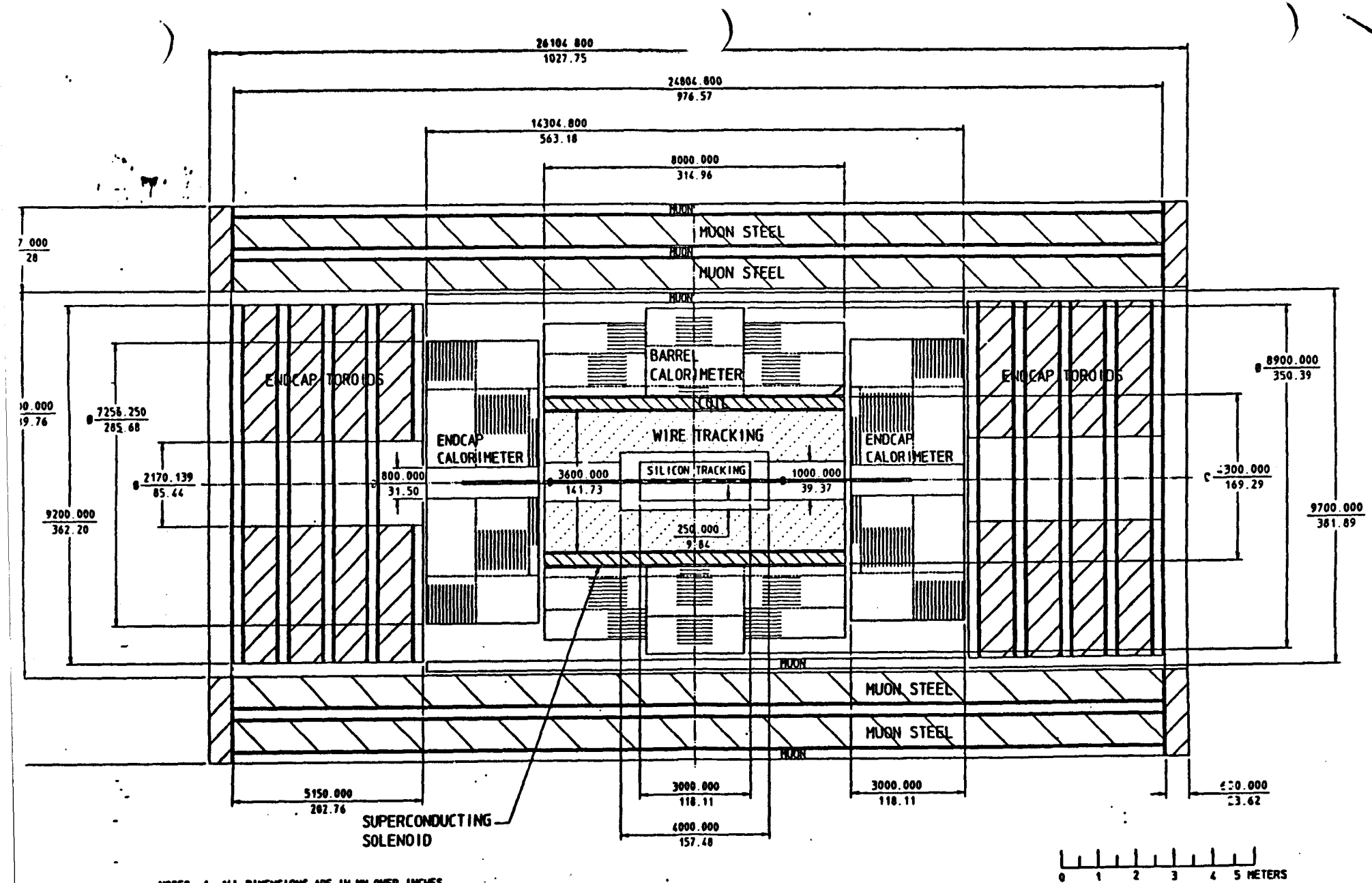

NOTES: 1. ALL DIMENSIONS ARE IN MM OVER INCHES.

SHORT COIL OPTION
SEPTEMBER 20, 1989

FIG 3

23 m

FIG4: FRACTIONAL CHANGE IN COLLECTED CHARGE VS. PSEUDO RAPIDITY

$\mathcal{L} = 10^{33}$

$V = 2\,KV$

$L = 1\,mm$

TMS

10^{-3}

10^{-4}

10^{-5}

10^{-6}

10^{-7}

1 2 3

rapidity

SEMI-LOGARITHMIC 5 CYCLES X 70 DIVISIONS AD-0045 -6T

GRAPH PAPER GRAPHIC CONTROLS CORPORATION Buffalo, New York

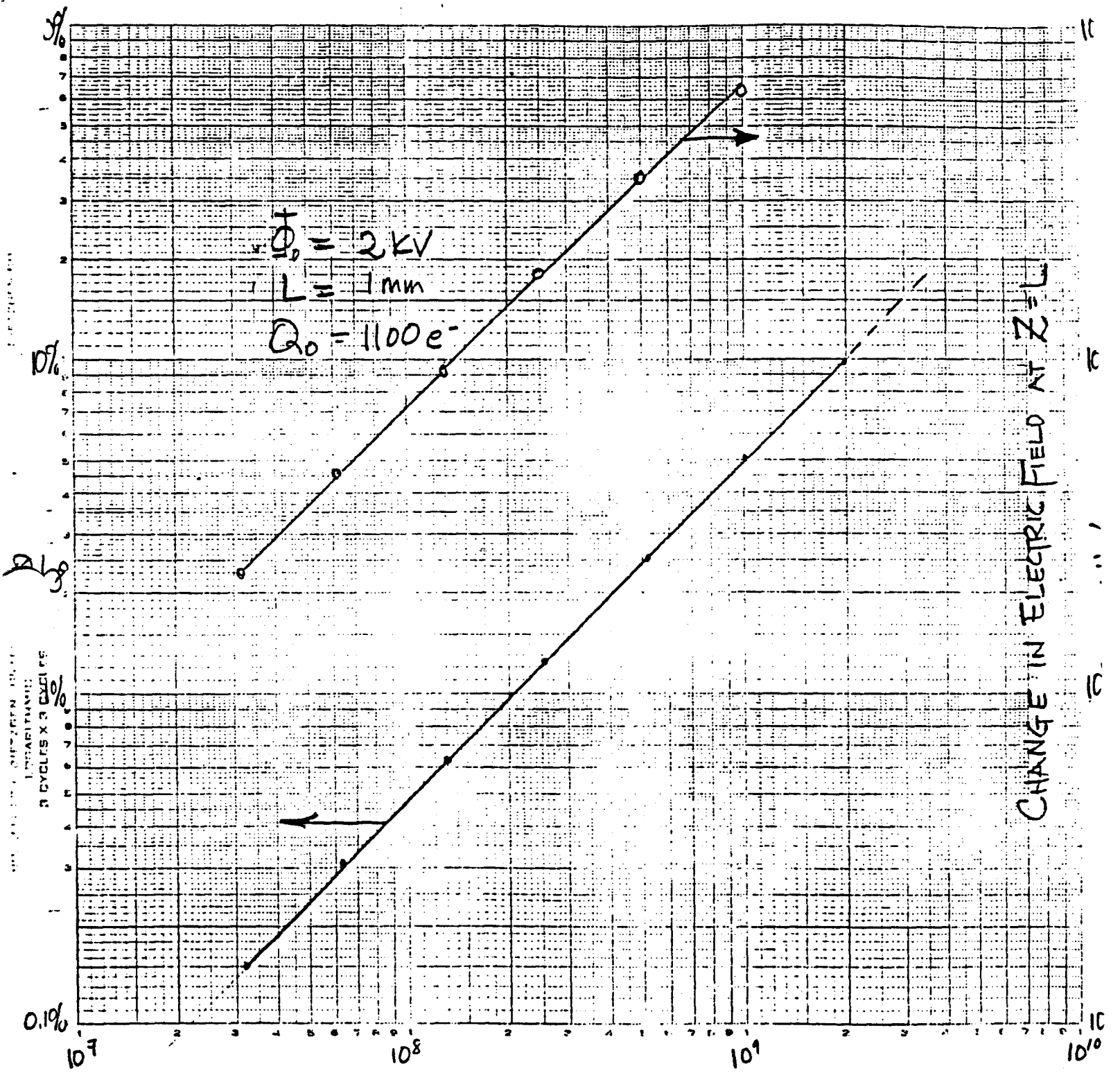

FIGURE 5: FRACTIONAL CHANGE IN COLLECTED CHARGE VS RATE OF MIN-IONIZING PARTICLES.

FIG 6.

PHOTON AND ELECTRON ATTENUATION

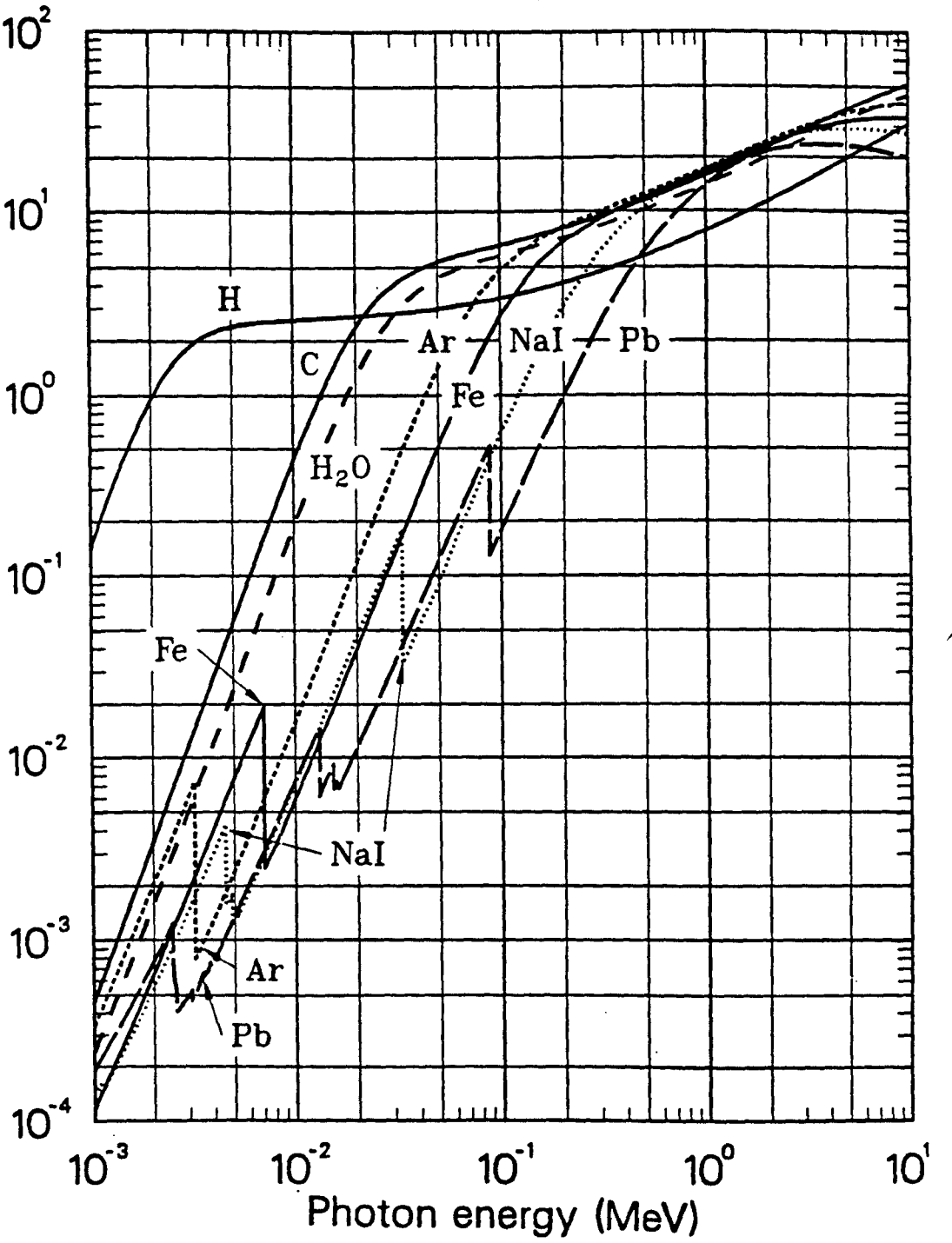

The photon mass attenuation length $\lambda = 1/(\mu/\rho)$ (also known as mfp, mean free path) for various absorbers as a function of photon energy, where μ is the mass attenuation coefficient. For a homogeneous medium of density ρ, the intensity I remaining after traversal of thickness t is given by the expression $I = I_0 \exp(-t\rho/\lambda)$. The accuracy is a few percent. Interpolation to other Z should be done in the cross section $\sigma = A/\lambda N_A$ cm^2/atom, where A is the atomic weight of the absorber material in grams and N_A is the Avogadro number. For a chemical compound or mixture, use $(1/\lambda)_{\text{eff}} \cong \sum w_i(1/\lambda)_i$, accurate to a few percent, where w_i is the proportion by weight of the i^{th} constituent. See next page for high energy range. The processes responsible for attenuation are given in the bottom figures of the next page. Not all of these processes necessarily result in detectable attenuation. For example, coherent Rayleigh scattering off an atom may occur at such low momentum transfer that the change in energy and momentum of the photon may not be significant. From Hubbell, Gimm, and Øverbø, J. Phys. Chem. Ref. Data 9, 1023 (1980). See also J.H. Hubbell, Int. J. of Applied Rad. and Isotopes 33, 1269 (1982). Data courtesy J.H. Hubbell.